

Single-Phase Photovoltaic (PV) Inverter Topology Consisting an Inductive Filter, and a Boost Converter Interfacing to the Grid

G.Mahesh

M.Tech Student,

Dept of EEE,

**Siddharth Institute of Engineering & Technology,
Puttur.**

K.Mani M.Tech

Assistant Professor,

Dept of EEE,

**Siddharth Institute of Engineering & Technology,
Puttur.**

ABSTRACT:

Generally the Power circuit topology of the single phase PV system will be a good choice for low-rated photo voltaic inverters of rating less than a kilowatt. In the ideal case the system will not have any lower order harmonics. However, some dominant factors result in lower order harmonics in the system such as on-state voltage drops across the switches and the distortion in the grid voltage itself etc. This dc injection into the primary of the transformer will result in even harmonics which are being drawn from the grid, again providing a lower power quality. In this work, a single-phase grid-connected photovoltaic inverter topology consists of a boost section, a low-voltage single-phase H-bridge inverter with an inductive filter, and a step-up transformer interfacing the grid is presented. A novel design of inverter current control that attenuates the lower order harmonics is presented in this project. An adaptive harmonic compensation technique with its design is proposed for the lower order harmonic compensation. In addition, a proportional-resonant-integral (PRI) controller and its design is also proposed. So, in this project some modification is made in the inverter current control for a grid connected single-phase photovoltaic inverter for ensuring high quality of the current to be injected into the grid. The proposed method uses an LMS (Least Mean Square) adaptive filter to estimate a particular harmonic content in the grid current that needs to be attenuated. The estimated current is converted into an equivalent voltage reference using an adaptive filter gain and added to the inverter voltage reference.

The entire system will be designed and tested using MATLAB/SIMULINK and Simulation results are used to confirm the performances of the Grid-Connected Single-Phase photovoltaic Inverter.

I. INTRODUCTION:

Now a days energy demand has been increasing day to day as the standard of living of people of any country is proportional to the energy consumption made by them. We know that basically there are two types of energy sources namely conventional energy sources and renewable energy sources. Renewable energy sources like solar, wind, and geothermal have gained popularity due to the depletion of conventional energy sources. Hence, many distributed generation (DG) systems making use of the renewable energy sources are being designed and connected to a grid. In this work, one such Distributed Generation system with solar energy as the source is considered. The solar inverter system topology consists of the following three power circuit stages:

- 1) A boost converter stage.
- 2) A single-phase H-bridge inverter.
- 3) A step-up transformer and inductive filter.

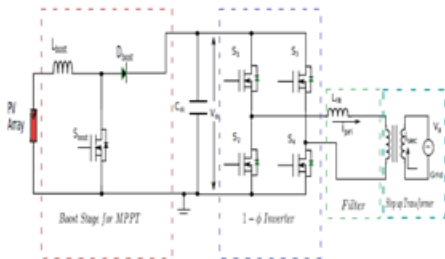


Fig1.1: Power circuit topology of the 1 – φ PV

System for a low-voltage inverter

The switches in Fig. 1 are rated for the low voltage which results in reduction of cost, the component count will be reduced and the overall reliability of the system enhances. The above circuit comprises of a low voltage inverter with 40v dc bus connected to 230v grid using step up transformer. This topology consists of a PV array which is a combination of eight PV panels; each panel consists of three modules and it is a good choice for low-rated PV inverters of rating less than a kilowatt. When compared to the other systems this topology has a relatively larger size of the interface transformer which is a disadvantage. Other topologies consist of a high-frequency link transformer. In the ideal case the system shown in Fig. 1 is free from lower order harmonics. However, the following factors will be dominant causes for the lower order harmonics in the system: The distorted magnetizing current drawn by the transformer due to the nonlinearity in the B–H curve of the transformer core, the dead time introduced between switching of devices of the same leg of the inverter, on-state voltage drops on the switches which causes same distortion as the dead time effect, and the distortion in the grid voltage itself. There can be a dc injection into the transformer primary due to a number of reasons. These may be the varying power reference from a fast MPPT block from which the ac current reference is generated which is given as reference for error detection, the offsets in the sensors, and A/D conversion block in the digital controller. This dc injection would result in even harmonics being drawn from the grid. It is important to attenuate these lower order harmonics in order for the PV inverter to meet standards such as

IEEE 519-1992 and IEEE 1547-2003. Hence, In this work we concentrate on the design of the inverter current control in order to achieve a good attenuation of the lower order harmonics. It must be observed that attenuating the lower order harmonics using a larger output filter inductance is not a good because it increases losses in the system along with a larger fundamental voltage drop and cost will be increased. This work includes an analysis to design the value of the gain in the proportional resonant controller to achieve an adequate level of harmonic compensation. The consequence of this scheme on the whole system dynamics is also analyzed. Adaptive filter method is simple for implementation and hence it can be implemented in a low-end digital controller. The presence of dc in the inverter terminal voltage results in a dc current flow into the primary of the transformer. This dc current results in drawing even harmonics from the grid. If the main controller used is a Proportional Resonant controller, any dc offset in a control loop will propagate through the system and the inverter terminal voltage will have a nonzero average value. Thus, in this work, a modification to the conventional PR controller scheme is proposed. An integral block is used along with the PR controller to ensure that there is no dc in the output current of the inverter. This would automatically eliminate the even harmonics. This scheme is termed as proportional-resonant-integral (PRI) control and the design of the PRI controller parameters are provided in this work. The objective of this work is to improve the power quality of the system with the inverter current control in order to attenuate the lower order harmonics. Improving the quality of current injected into the grid is the main aim of the thesis.

II. PHOTOVOLTAIC SYSTEMS

Converting solar energy into electrical energy by PV installations is the most acknowledged way to use solar energy. Since solar photovoltaic cells are layers of semiconductor devices, they have a lot in common with processing and production techniques of other semiconductor devices such as computers and memory

chips. As it is well known that the requirements for purity and quality control of semiconductor devices are quite prominent. Today's production reached a large scale, the whole industry production of solar cells has been developed and, due to low production cost, it is mostly located in the Far East. Photovoltaic cells produced by the majority of today's most large producers are mainly made of crystalline silicon as semiconductor material. Solar photovoltaic modules, which are a result of combination of photovoltaic cells to increase their power, reliability, durability and reduce noise while producing electricity. The fuel for the photovoltaic cell is free. The sun is the only resource that is required for the operation of PV systems, and its energy is unlimited. Typical photovoltaic cell efficiency is about 15%, which means it can convert 1/6 of solar energy into electricity. Photovoltaic systems do not produce noise, and there are no moving parts and they do not emit pollutants into the environment. Taking into account the energy consumed in the production of photovoltaic cells, they produce several times less carbon dioxide per unit in relation to the energy produced from fossil fuel technologies. Photovoltaic cell has a lifetime of more than thirty years and is one of the most reliable semiconductor products. Most solar cells are produced from silicon, which is non-toxic and is found in abundance in the earth's crust.

FUNCTIONING OF PHOTOVOLTAIC CELLS

The word photovoltaic consists of two words: photo, a Greek word for light, and voltaic, which defines the measurement value by which the activity of the electric field is articulated. Photovoltaic systems use PV cells to renovate sunlight into electricity. Photovoltaic installation is the most popular way. The light has a dual character according to quantum physics. Light is a particle and it is a wave. The particles of light are called photons. Photons are mass less particles, moving at light speed. The energy of the photon depends on its wavelength and the frequency, and we can calculate it by the Einstein's law, which is given as follows

$$E = hv \dots\dots\dots 2.1$$

From the above equation,

E represents the photon energy and h represents the Planck's constant h
 $= 6.626 \times 10^{-34} Js \dots\dots\dots 2.2$

In general electrons either exist as valence or free in case of metals and in matter. Valence electrons are related with the atom, while the free electrons are separated from the atom and they can move. In order for the valence electron to become separate from the atom, it should get the energy that is greater than or equal to the binding energy. Binding energy is the energy by which an electron is bound to an atom in one of the atomic bonds. In case of photovoltaic effect, the electron gets the required energy by the collision with a photon. some of the photon energy is used for the electron getting free from the influence of the atom which it is attached to, and the remaining energy is converted into kinetic energy of a now free electron. Free electrons obtained by the photoelectric effect are also called photoelectrons. The energy required to release a valence electron from the impact of an atom is called a work out W_i , and it depends on the type of material in which the photoelectric effect has occurred. The equation that describes this process is as follows:

$$hv = W_i + E_{kin} \dots\dots\dots 2.3$$

In the above equation, hv represents the photon energy, W_i represents the work out and E_{kin} represents the kinetic energy of emitted electron. The equation 2.3 shows that the electron will be released if the photon energy is less than the work output. The photoelectric conversion in the PV junction. PV junction (diode) is a boundary between two differently doped semiconductor layers; one is a P-type layer (excess holes), and the second one is an N-type. At the margin between the P and the N area, there is a spontaneous electric field, The generated electrons and holes are affected by the electric field and it is possible to determine the direction of the current.

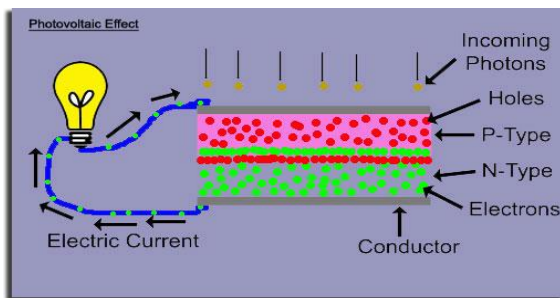


Fig 2.1: Functioning of PV cell

To obtain the energy by the photoelectric effect, there shall be a directed motion of photoelectrons. All charged particles along with the photoelectron will move in a directed motion under the influence of electric field. In case of any material the electric field will be located itself in semiconductors, specifically in the poor area of PV junction (diode). It was pointed out in case of the semiconductors that, in company with the free electrons in them, there are cavities as charge carriers, which are a sort of a consequence in the emergence of free electrons. Cavities occurs whenever the valence electron turns into a free electron, and this process is called the generation, whereas the reverse process, when the free electron fills the empty spaces - a cavity, is called recombination. If the electron-cavity pairs occur away from the impoverished areas it is possible to recombine before they are separated by the electric field. Photoelectrons and cavities in semiconductors are accumulated at opposite ends, thereby creating an Electro Motive Force. If a intense device is connected to such a system, the current will flow through it and we will get electricity.

PHOTOVOLTAIC MODULE

The power produced by a single PV cell is not enough for general use. So by connecting many single PV cell in series (for high voltage requirement) and in parallel (for high current requirement) can get us the desired power. Generally a series connection is chosen this set of arrangement is known as a module. Generally commercial modules consist of 36 or 72 cells. The modules consist of transparent front side, encapsulated PV cell and back side. The front side material is

generally made up of low-iron and tempered glass. The efficiency of a Photo Voltaic module is less than a Photo Voltaic cell. This is due to the fact that some radiation is reflected by the glass cover and frame shadowing etc.

2.5 PHOTOVOLTAIC ARRAY

A photovoltaic array (PV system) is an interconnection of modules which in turn is made up of many PV cells connected in series or parallel. The power generated by a one module is hardly ever enough for commercial use, so PV modules are connected to form an array to supply the load. The connection of the modules in an array is same as that of cells in a module. Modules are usually connected in series to get an increased voltage or in parallel to get an increased current. In urban uses, generally the arrays are mounted on a rooftop. In agricultural use, the output of an array can directly feed a DC motor.

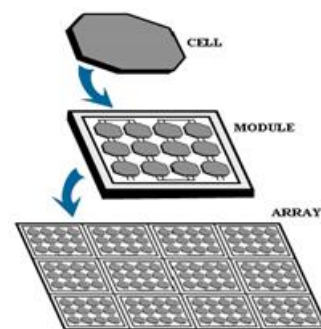


Fig 2.2 Photovoltaic Hierarchy

CHARACTERISTICS OF A PV CELL:

In a PV characteristic there is basically three important points viz. open circuit voltage, short circuit current and maximum power point. The maximum power that can be extracted from a PV cell are at the maximum power points. Usually manufacturers provide these parameters in their datasheets for a particular PV cell or module. By using these parameters we can build a simple model but for more information is required for designing an accurate model.

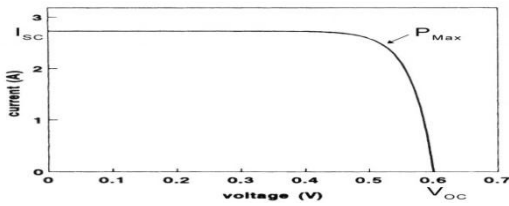


Fig 2.3 Characteristics of a PV cell

2.7 CATEGORIES OF PV SYSTEMS:

- 1) Simple or "Stand Alone" PV Systems
- 2) PV with Battery Storage
- 3) PV systems with endorsement Generator power
- 4) PV system Connected to the Local Utility
- 5) Efficacy-Scale Power Production
- 6) Hybrid Power Systems

PERTURB AND OBSERVE ALGORITHM

The P&O algorithm is also called "hill-climbing", but both names belong to the same algorithm depending on how it is enforced. Hill-climbing implies a perturbation on the duty cycle of the power converter and P&O a perturbation in the operating voltage of the DC link between the PV array and the power converter. In the case of the Hill-climbing, disturbing the duty cycle of the power converter implies modifying the voltage of the DC link between the PV array and the power converter, so both the names belong to the same technique. In this method, the sign of the last perturbation and the sign of the last increment in the over are used to decide what the next perturbation should be. As can be seen in Figure, on the left of the MPP incrementing the voltage increases the power whereas on the right decrementing the voltage increases the power.

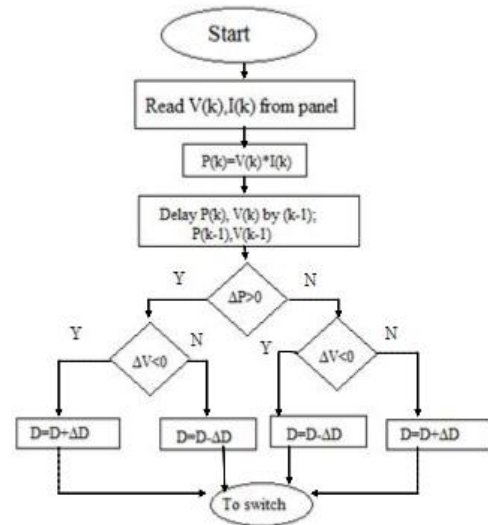


Fig: 2.5 perturb & observe algorithm with duty cycle

P&O algorithm is based on the calculation of the PV array output power and the power change by sensing both the PV current and voltage. The controller operates occasionally by comparing the present value of the power output with the previous value to determine the change on the solar array voltage or current. The algorithm reads the values of current and voltage at the output solar PV module. Power is calculated from the considered voltage and current. The magnitudes of voltage and power at k^{th} instant are stored. Then the magnitudes of power and voltage at $(k+1)^{th}$ instant are measured again and power is calculated from the measured values.



Fig: 2.6 perturb & observe algorithm with voltage reference

If the magnitude of power is rising, the perturbation will persist in the same direction in the next cycle, if not the perturbation direction is inverted. When the MPP is reached, the system after that oscillates around the MPP. In order to diminish the oscillation, the disruption step size should be reduced such that when the operating point is away from the MPP, the step alteration in duty cycle should be huge, when it nears the MPP, the step change in 'α' should reduce. In figure 2.6 the perturb and observe algorithm is based on the voltage reference is illustrated. First of all we have to calculate the voltage and current at the instant k and then calculate the change in voltage and current i.e. ΔV and ΔI. we need to check the condition ΔV = 0, If this condition satisfies we will check another condition ΔI = 0. If the condition ΔI = 0 is not satisfied then check the condition ΔI > 0 if this is satisfied then the voltage reference will be decreased otherwise the voltage reference is increased. If the condition ΔV = 0 is not satisfied then check the condition $I + \frac{\Delta I}{\Delta V} V = 0$ if this condition is satisfied then check other condition $I + \frac{\Delta I}{\Delta V} V > 0$ if it is yes then the voltage reference is decreased otherwise voltage reference will be increased.

3. HARMONICS

A sinusoidal element of a periodic wave or quantity having a frequency that is an integral multiple of fundamental frequency is called as harmonics. Harmonics are multiples of a fundamental frequency. In music, they are known as octaves, and are usually advantageous. But in a plant's electrical power distribution system, they are unnecessary. Harmonics cause trouble when combined with the fundamental electrical waveform. As these harmonics are multiples of the 60-Hz fundamental power frequency. Harmonic frequencies can be two times at 120-Hz frequency, three times at 180-Hz frequency, and soon. When harmonics mix with the fundamental, they distort the sine wave (Fig.3.1). Any distorted /truncated waveform can be analyzed by Fourier series to obtain a

multitude of frequencies, superimposed upon on another.

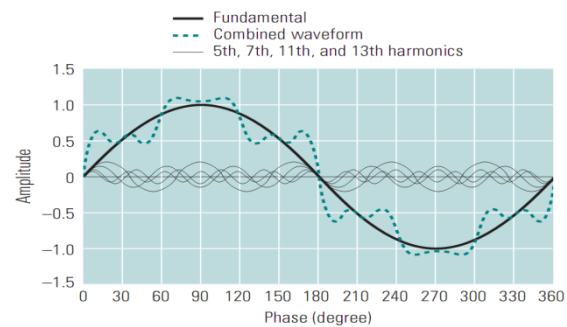


Fig: 3.1 Effect of harmonics on normal voltage or current waveform

3.2 TOTAL HARMONIC DISTORTION (THD)

IEEE defines harmonic content as "a measure of the presence of harmonics in a voltage or current waveform expressed as a percentage of the amplitude of the fundamental frequency at each harmonic frequency. The total harmonic content is articulated as the square root of the sum of the squares of each of the harmonic amplitudes." It is defined in the Institute of Electrical and Electronic Engineers (IEEE) standard 519-1992 as the ratio of RMS square values of all harmonics to the RMS square values of the fundamental. It is given by the formula.

$$\%THD = \frac{(\text{sum of squares of amplitudes of all harmonics})^{1/2}}{(\text{square of amplitude of fundamental}) \times 100}$$

$$\%THD = \sqrt{\frac{V_n^2}{V_1^2}} \times 100 \dots \dots 3.1 \text{ Where, } n = 2, 3,$$

V_1 = Fundamental Voltage

I_{THD} is called current harmonic distortion

V_{THD} is called voltage harmonic distortion.

Harmonic distortion adds overtones that are whole number multiples of a sound wave's frequencies. Nonlinearities that give rise to amplitude distortion in audio systems are most often measured in terms of the

harmonics (overtones) added to a pure sine wave fed to the system. Harmonic distortion may be articulated in terms of the relative strength of entity components, in decibels, or the Root Mean Square of all harmonic components: Total harmonic distortion (THD), as a percentage. The level at which harmonic distortion becomes audible is not straightforward. Different types of distortion (like crossover distortion) are more audible than others (like soft clipping) even if the THD measurements are the same. Harmonic distortion in RF applications is rarely expressed as THD.

3.3 SOURCES OF HARMONIC DISTORTION

Non-linear equipment or components in the power system cause distortion of the current and to a lesser extent of the voltage. These sources of distortion can be divided in three groups:

1. loads
2. the power system itself (HVDC, SVC, transformers, etc)
3. the generation stage (synchronous generators)

Subdivision can also be made regarding the connection at different voltage levels. Usually, loads can be considered connected at lower voltage levels, the power system exists at every voltage level and the generation stage at low and medium voltage levels. The dominating distortion-producing assemblies, worldwide, are the loads. At some locations HVDC-links, SVC's, arc furnaces and wind turbines contributes more than the other sources. The generation stage can, during some special conditions, contribute to some voltage distortion at high voltage transmission stage. The attribute behavior of non-linear loads is that they draw a distorted current waveform even though the supply voltage is sinusoidal. Most apparatus only produces odd harmonics but some devices have a fluctuating power consumption, from half cycle to half cycle or shorter, which then generates odd, even and inter harmonic currents. The current distortion, for each device, changes due to the consumption of active power, background voltage distortion and alterations in the

source impedance. In this chapter an overview will be given of the most common types of current waveforms from single and three phase non-linear loads for residential and industrial use. Most of the waveforms are obtained from field dimensions. regulates on the current distortion of the supply voltage background distortion and fundamental voltage unbalance are also addressed.

3.3.1 SINGLE PHASE LOADS

Electronic equipment, supplied from the low voltage power system, rectifies the ac power to dc power for internal use at different dc voltage levels. This is done, with or without an ac step down transformer, and a diode rectifier. The dc voltage is smoothed by a dc capacitor. The power range for each device is little, from a few Watts up to some kilo Watts. The total harmonic distortion, THD, of the line current is often over 100 % and consists of all odd multiples of the fundamental component. In some case the THD can be nearly 150 %, mainly depending on the design of the DC-link and the crest factor of the supply voltage. This group is utilized both by households and by production. It comprises of:

- TV's
- Video recorders
- Computers
- Printers
- Micro wave ovens
- Adjustable speed drives (low power)
- H.F. fluorescent lighting
- Small UPS's

SINGLE PHASE INVERTERS:

The dc-ac converter, also known as the inverter, converts dc power to ac power at belovod output voltage and frequency. The dc power input to the inverter is given from an existing power supply network or from a rotating alternator through a rectifier or a battery, fuel cell, PV array or magneto hydrodynamic generator.

The capacitive filter across the input terminals of the inverter provides a constant dc link voltage. The inverter therefore is an regulating-frequency voltage source. The design of ac to dc converter and dc to ac inverter is called a dc-link converter. Inverters can be generally classified into 2 types, voltage source and current source inverters. A voltage-fed inverter (VFI) or more generally a voltage-source inverter (VSI) is one in which the dc source has small or insignificant impedance. The voltage at the input terminals is constant. A current-source inverter (CSI) is fed with adjustable current from the dc source of high impedance that is from a constant dc source. A voltage source inverter employing thyristors as switches, some type of forced commutation is necessary, while the VSIs made up of utilising GTOs, power transistors, power MOSFETs or IGBTs, natural commutation with base or gate drive signals for their controlled turn-on and turn-off. A standard single-phase voltage or current source inverter can be in the half-bridge or full-bridge configuration. The single-phase units can be attached to have three-phase or multiphase systems. Some industrial applications of inverters are for variable-speed ac drives, induction heating, stand-in aircraft power supplies etc.

3.3.2.1 Voltage Control in Single - Phase Inverters:

The schematic of inverter system is as shown in Figure 3.2, in which the battery or rectifier provides the dc supply to the inverter. The inverter is utilized to control the fundamental voltage magnitude and the frequency of the ac output voltage. AC loads may need constant or adjustable voltage at their input terminals, when such type of loads are fed by inverters, it is necessary that the output voltage of the inverters is so controlled as to fulfill the requirement of the loads. For instance if the inverter supplies power to a magnetic system like an induction motor, the voltage to frequency ratio at the inverter output terminals must be kept constant. This prevents saturation in the magnetic circuit of the device fed by the inverter.

The different methods for the control of output voltage of inverters can be classified as:

- a) External control of the ac output voltage
- b) External control of the dc input voltage
- c) (c) Internal control of the inverter.

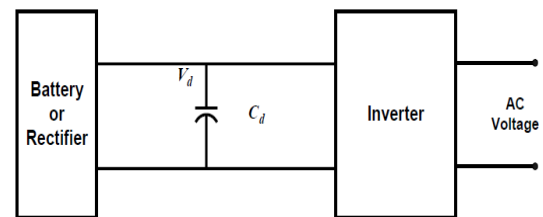


Figure3.2: Schematic for Inverter System

The earliest two methods require the use of peripheral components whereas the third method requires no external components.

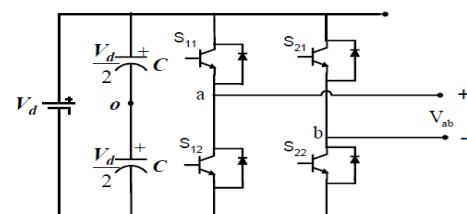


Figure 3.3: Schematic of a Single Phase Full-Bridge Inverter.

A single-phase inverter in the full bridge topology is as shown in Figure3.3, which consists of four switching devices, two of the four switches are on each leg. The full-bridge inverter can produce an output power twice that of the half-bridge inverter with the same input voltage. Three dissimilar PWM switching schemes are generally used, which improve the characteristics of the inverter. The aim is to add a zero sequence voltage to the modulation signals in such a way to ensure the clamping of the devices to either the positive or negative dc rail; in the process of which the voltage gain is enhanced, leading to an increased load

fundamental voltage, decline in total current distortion and increased load power factor.

3.4.1.2 Inverter dead time effect

The dead-time effect introduces lower order harmonics which are proportional to the dead time, switching frequency, and the dc bus voltage. The dead-time effect for each leg of the inverter can be modeled as a square wave error voltage out of phase with the current at the pole of the leg. The device drops also will cause a similar effect but the resulting amount of distortion is smaller compared to that due to the dead time. Thus, for a single-phase inverter topology considered, net error voltage is the voltage between the poles and is out of phase with the primary current of the transformer. The harmonic voltage amplitude for a h^{th} harmonic can be expressed as

$$V_{error} = \frac{4}{h\pi} \frac{2V_{dc} t_d}{T_s}$$

where t_d is the dead time, T_s is the device switching frequency, and V_{dc} is the dc bus voltage. Using the values of the filter inductance, transformer leakage inductance, and the net series resistance, the harmonic current magnitudes can be evaluated. Again, it must be noted that the phase angle of the harmonic currents in this case will be 180° for UPF operation. Thus, it can be observed that the net harmonic content will have some phase angle with respect to the fundamental current depending on the relative magnitudes of the distortions due to the magnetizing current and the dead time.

INTRODUCTION TO THE PRI CONTROLLER:

Conventional stationary reference frame control consists of a PR controller to generate the inverter voltage reference. In this work, an adjustment to the PR controller is proposed, by adding an integral block, G_I as indicated in Fig.3.7. The modified control structure is termed as a PRI controller. Here ,

$$G_I = \frac{K_I}{s} \dots\dots\dots 3.3$$

$$G_{PR}(s) = K_p + \frac{K_r s}{s^2 + \omega_0^2} \dots\dots\dots 3.4$$

Proportional integral controller is the most widely used controller but it consists of a zero at the fundamental frequency hence, it is not possible to eliminate the steady state error. In case of proportional resonant controller, at resonant frequency the gain will be increased and error will be reduced.

The plant transfer function can be written as follows

$$G_{plant}(s) = \frac{V_{dc}}{R_s + sL_s} \dots\dots\dots 3.5$$

This is because the inverter will have a gain of V_{dc} to the voltage reference generated by the controller and the impedance offered is given by $(R_s + sL_s)$ in s-domain. R_s and L_s are the net resistance and inductance referred to the primary side of the transformer, respectively. L_s includes the filter inductance and the leakage inductance of the transformer. R_s is the net series resistance due to the filter inductor and the transformer. The PRI controller is proposed to ensure that the output current of the system does not contain any dc offset. The PRI controller introduces a zero at $s = 0$ in the closed-loop transfer function. Hence, the output current will not contain any steady state dc offset. This is necessary in the topology considered because the presence of a dc offset would result in a flow of even harmonics. The following section explains the design of PR controller parameters and proposes a systematic method of selecting and tuning the gain of the integral block in the PRI controller.

3.5.2 DESIGN OF PRI CONTROLLER PARAMETERS:

The fundamental current corresponds to the power injected into the grid. The control objective is to achieve unity power factor (UPF) operation of the inverter. The main control block diagram is shown in Fig.3.7. First, a PR controller is designed for the system assuming that the integral block is absent, i.e., $K_i = 0$.

Design of a PR controller is done by considering a PI controller in place of the PR controller. The PI parameters are chosen based on the plant transfer function and the required current controller bandwidth. The PI controller parameters are then plugged in for the PR controller parameters.

$$\text{Let } G_{PI} = K_{p1} \frac{1+sT}{sT} \quad \dots\dots\dots 3.6$$

With the PI controller as the compensator block in Fig.3.7 and without integral block, the forward transfer function will be

$$G_{\text{forw}}(s) = \left(K_{p1} \frac{1+sT}{sT} \right) \frac{V_{dc}}{R_s + L_s} \quad \dots\dots\dots 3.7$$

The pole in the above equation is canceled with the zero given by the PI controller. Then, the following relations are obtained:

$$T = \frac{L_s}{R_s} \quad \dots\dots\dots 3.8 \quad G_{\text{forw}}(s) = \frac{K_{p1} V_{dc}}{sT R_s} \quad \dots\dots\dots 3.9$$

If W_{bw} is the required bandwidth, then K_{p1} can be selected to be

$$K_{p1} = \frac{\omega_{bw} R_s T}{V_{dc}} \quad \dots\dots\dots 3.10$$

Now, if the PI controller in equation 3.6 is written as

$$G_{p1}(s) = k_{p1} + \frac{K_{i1}}{s} \quad \dots\dots\dots 3.11$$

Then, K_{i1} is given as

$$K_{i1} = \frac{\omega_{bw} R_s}{V_{dc}} \quad \dots\dots\dots 3.12$$

For the PR controller, the expressions obtained in equations 3.10 and 3.12 are used for the K_p and k_r respectively.

$$\text{Hence, } K_p = \frac{\omega_{bw} R_s T}{V_{dc}} \quad \dots\dots\dots 3.13 \quad k_r = \frac{\omega_{bw} R_s}{V_{dc}} \quad \dots\dots\dots 3.14$$

For the complete system with an integral block, i.e., the PRI controller, the PR parameters will be same as in equations 3.13 and 3.14. The following procedure is used to select the value of K_i in equation 3.3. The integral portion is used to ensure that there will not be any steady-state dc in the system. Hence, the overall dynamic performance of the complete system should be similar to that with the PR controller except at the low-frequency region and dc.

The closed-loop transfer function for Fig.3.7 is given as, $G_{cl,PRI} = \frac{i(s)}{i^*(s)}$

$$= \frac{G_{\text{plant}} G_{PR}}{1 + G_{\text{plant}} (G_{PR} + G_{PI})} \quad \dots\dots\dots 3.15$$

Without the integral block, the closed-loop transfer function would $G_{cl,PR} = \frac{G_{\text{plant}} G_{PR}}{1 + G_{\text{plant}} G_{PR}} \quad \dots\dots\dots 3.16$

Let 3.4 be modified as

$$G_{\text{plant}} = \frac{M}{1+sT} \quad \dots\dots\dots 3.17$$

Where $M = V_{dc}/R_s$ and T is as defined in equation 3.9. The numerators in both equations 3.15 and 3.16 are the same. Thus, the difference in their response is only due to the denominator terms in both. The denominator in equation 3.15 can be obtained as

$$\text{den}_{PRI} = \left[\frac{T^2 s^4 + (1 + MK_p) s^3 + (\omega_0^2 T + M(K_r + K_I)) s^2 + s(MK_p + 1)\omega_0^2 + MK_I \omega_0^2}{s(1+sT)(s^2 + \omega_0^2)} \right] \quad \dots\dots 3.18$$

Similarly, the denominator in equation 3.16 is given by

$$\text{den}_{PR} = \left[\frac{T^2 s^3 + (1 + MK_p) s^2 + (\omega_0^2 T + MK_r) s + (MK_p + 1)\omega_0^2}{(1+sT)(s^2 + \omega_0^2)} \right] \quad \dots\dots 3.19$$

The numerators in equations 3.18 and 3.19 are the characteristic polynomials of the closed-loop transfer functions given in equations 3.15 and 3.16, respectively. Let the numerator polynomial in equation 3.18 be written as

$$(s + p)(as^3 + bs^2 + cs + d) = as^4 + (b + ap) s^3 + (c + bp) s^2 + (d + cp)s + dp \quad \dots\dots 3.20$$

where p corresponds to a real pole

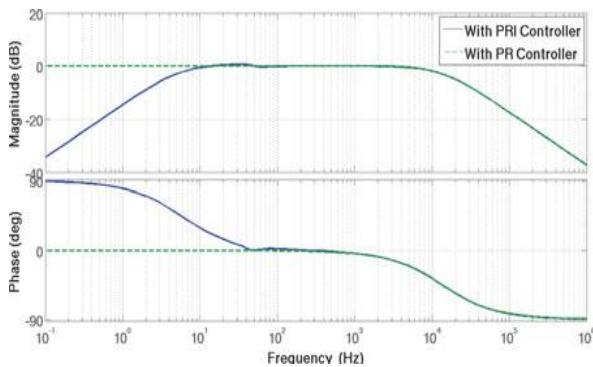


Fig.3.8. Comparison of a Bode plot of the closed-loop transfer function with the PRI ($G_{cl,PRI}$) and PR controllers ($G_{cl,PR}$).

If p is such that it is very close to the origin and the remaining three poles in equation 3.15 are as close as possible to the poles of equation 3.16, then the reaction in case of the PRI controller and the PR controller will be very similar except for dc and low frequency range. Consequently, the remaining third-order polynomial in equation 3.20 should have the coefficients very close to the coefficients of the numerator in equation 3.19.

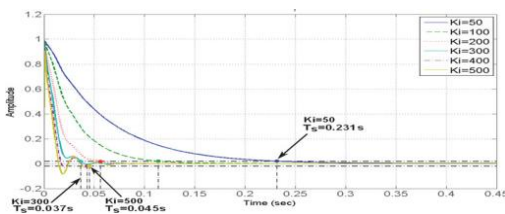


Fig.3.9. Step response of closed-loop transfer function $G_{cl,PRI}$ for different values of K_I .

Thus, 3.22–3.23 can be used to design the value of K_I . Fig.3.8 shows the comparison between the Bode plots of the system with the PRI and PR controllers validating the design procedure for the given values. As it can be observed, the responses differ only in the low frequency range.

The system with the PRI controller has zero gain for dc while the system with the PR controller has a gain of near unity. The step response of the closed-loop system with the PRI controller can be seen in Fig. 3.9. As can be observed, increasing K_I has an effect of decreasing the settling time up to a certain value. Beyond that, the system becomes under damped and settling time increases with increase in K_I . This plot can be used to tune the value of K_I further.

4. ADAPTIVE HARMONIC COMPENSATION

4.1 LMS ADAPTIVE FILTER:

The adaptive harmonic compensation technique is based on the usage of an LMS adaptive filter to estimate a particular harmonic in the output current. This is then used to generate a counter voltage reference using a proportional controller to attenuate that particular harmonic. Adaptive filters are commonly used in signal processing applications to remove a particular sinusoidal interference signal of known frequency. Fig.4.1 shows a general adaptive filter with N weights. The weights are modified by making use of the LMS algorithm.

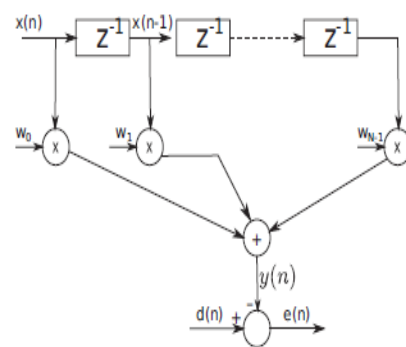


Fig.4.1. Structure of a generalized adaptive filter with adaptation weights w_i .

For Fig.4.1, coefficient vector is defined as

$$\bar{w} = [w_0 \ w_1 \ \dots \ w_{N-1}]^T$$

Vector input is given as follows

$$\bar{x}(n) = [x(n) \ x(n-1) \ \dots \ x(n-N+1)]^T$$

The error signal is

$$e(n) = d(n) - y(n) \quad \dots\dots\dots 4.1$$

Here, $d(n)$ is the primary input. A frequency component of $d(n)$ is adaptively expected by $y(n)$. Now, a performance function is defined for the LMS adaptive filter as

$$\zeta = e^2(n) \quad \dots\dots\dots 4.2$$

In any adaptive filter, the weight vector w is updated such that the performance function moves toward its minimum. Thus

$$\bar{w}(n + 1) = \bar{w}(n) - \mu \nabla(e(n)^2) \quad \dots\dots\dots 4.3$$

In 4.3, μ is the step size. The convergence of the adaptive filter depends on the step size μ . A smaller value would make the adaptation process very slow whereas a large value can make the system oscillatory. ∇ is defined as the gradient of the performance function with respect to the weights of the filter.

$$\bar{w}(n + 1) = \bar{w}(n) + 2\mu e(n)\bar{x}(n) \dots\dots\dots 4.4$$

Thus, from a set of known input vector $x(n)$, a signal $y(n)$ is obtained by the linear combination of $x(n)$ and the weight vector $w(n)$ as in 4.1. Signal $y(n)$ is an estimate of the signal $d(n)$ and the weight vector is continuously updated from 4.5 such that the LMS error $e(n) = d(n) - y(n)$ is minimized. This concept can be used to estimate any desired frequency component in a signal $d(n)$. The adaptive filter used for this purpose will take the reference input $x(n)$ as the sine and cosine terms at that desired frequency. The weight vector will contain two components which scale the sine and cosine and add them up to get an estimated signal $y(n)$. The weights will then be adapted in such a way as to minimize the LMS error between $d(n)$ and $y(n)$. In steady state, estimated signal $y(n)$ will equal the frequency component of interest in $d(n)$.

4.2 LMS ALGORITHM

The least-mean-square (LMS) is a search algorithm in which a simplification of the gradient vector computation is made possible by appropriately modifying the objective function. The LMS algorithm, as well as others related to it, is widely used in various applications of adaptive filtering due to its computational simplicity. The convergence characteristics of the LMS algorithm are examined in order to establish a range for the convergence factor that will guarantee stability. The convergence speed of the LMS is shown to be dependent on the Eigen value spread of the input signal correlation matrix. In this chapter, several properties of the LMS algorithm are discussed including the miss adjustment in stationary and non stationary environments and tracking performance. The analysis results are verified by a large number of simulation examples. The LMS algorithm is by far the most widely used algorithm in adaptive filtering for several reasons. The main features that attracted the use of the LMS algorithm are low computational difficulty, proof of convergence in a standstill environment, unbiased convergence in the mean to the Wiener solution, and steady behavior when implemented with finite-precision arithmetic. The overlap analysis of the LMS presented here utilizes the independence postulation. We have already derived the optimal solution for the parameters of the adaptive filter implemented through a linear combiner, which corresponds to the case of multiple input signals. This solution leads to the minimum mean-square error in estimating the reference signal $d(k)$. The optimal (Wiener) solution is given by

$$W_0 = R^{-1}p \quad \dots\dots\dots 4.5$$

Where, $R = E[x(k)X^T(k)]$ and $p = E[d(k)x(k)]$, assuming that $d(k)$ and $x(k)$ are jointly wide-sense stationary. If good estimates of matrix R , denoted by $\hat{R}(k)$, and of vector p , denoted by $\hat{p}(k)$, are available, an algorithm can be used to search the Wiener solution of equation as follows:

$$w(k + 1) = w(k) + 2\mu(\hat{p}(k) - R(k)w(k)) \dots\dots\dots 4.6$$

For $k = 0, 1, 2, \dots$. Where $\hat{g}w(k)$ represents an estimate of the gradient vector of the objective Function with respect to the filter coefficients. One possible solution is to estimate the gradient vector by employing instantaneous estimates. By utilizing and employing the estimates we can generate a solution and gradient vector. The consequential gradient estimate can also be calculated. The consequential gradient estimate is given by

$$\hat{g} w(k) = -2d(k)x(k) + 2x(k)X^T(k)w(k)$$

By simplifying the above equation we get the followin $= -2e(k)x(k) \dots\dots\dots 4.7$

Note that if the objective function is replaced by the instantaneous square error $e^2(k)$, instead of the MSE, the above gradient estimate represents the true gradient vector since

$$\begin{aligned} \frac{\partial e^2(k)}{\partial w} &= [2e(k) \frac{\partial e(k)}{\partial \omega_0(k)} \quad 2e(k) \frac{\partial e(k)}{\partial \omega_1(k)} \quad \dots \quad 2e(k) \frac{\partial e(k)}{\partial \omega_N(k)}]^T \\ &= -2 e(k) x(k) \\ &= \hat{g} w(k) \end{aligned}$$

The resulting gradient-based algorithm is known as the least-mean-square algorithm, whose equation is

$$w(k + 1) = w(k) + 2\mu e(k)x(k) \dots\dots\dots 4.8$$

Where the convergence factor μ should be chosen in a range to guarantee convergence. Fig.4.2 depicts the realization of the LMS algorithm for a delay line input $x(k)$. Typically, one iteration of the LMS requires $N + 2$ multiplications for the filter coefficient updating and $N + 1$ multiplications for the error generation. It should be noted that the initialization is not necessarily performed as described in Algorithm, where the coefficients of the adaptive filter were initialized with zeros.

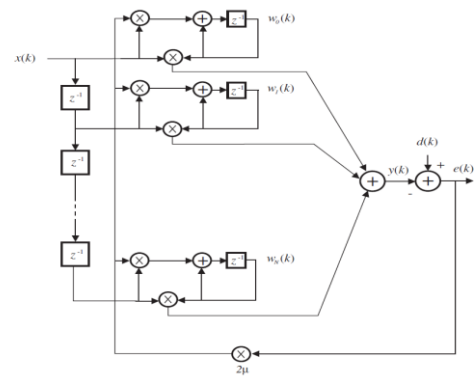


Figure 4.2: LMS adaptive FIR filter

4.3 ADAPTIVE HARMONIC COMPENSATION

The LMS adaptive filter discussed previously can be used for selective harmonic compensation of any quantity, say grid current. To reduce a particular lower order harmonic (say i_k) of grid current:

- 1) i_k is estimated from the samples of grid current and phase locked loop (PLL) unit vectors at that frequency;
- 2) a voltage reference is generated from the estimated value of i_k ;
- 3) generated voltage reference is subtracted from the main controller voltage reference.

Fig.4.3 shows the block diagram of the adaptive filter that estimates the k^{th} harmonic i_k of the grid current i . The adaptive block takes in two inputs $\sin(k\omega_0 t)$ and $\cos(k\omega_0 t)$ from a PLL. These samples are multiplied by the weights W_{cos} and W_{sin} . The resultant is subtracted from the perceived grid current sample, which is taken as the error for the LMS algorithm. The weights are then updated as per the LMS algorithm and the output of this filter would be an estimate of the k^{th} harmonic of grid current. The weights update would be done by using the equations given next, where T_s is the sampling time and μ is the step size

$$e(n) = i(n) - \hat{i}_k(n) \dots\dots\dots 4.9$$

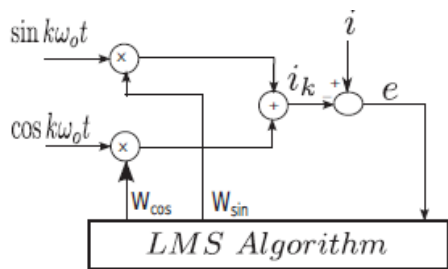


Fig.4.3. Block diagram of adaptive estimation of a particular harmonic of grid current.



Fig. 4.4. Generation of voltage reference from estimated kth harmonic component.

$$W_{\cos}(n+1) = W_{\cos}(n) + 2\mu e(n)\cos(k\omega_0 nT_s)$$

$$W_{\sin}(n+1) = W_{\sin}(n) + 2\mu e(n)\sin(k\omega_0 nT_s) \quad 4.10$$

Now, a voltage reference has to be generated from this estimated current. In this paper, the proportional gain method is used as it is very simple for both design and implementation and is verified to meet harmonic requirements. The overall current control block diagram with the adaptive compensation is shown in Fig. 4.5. Note that the fundamental current control is done using the transformer primary current and the harmonic compensation block uses the secondary current, which is the current injected into the grid. Fig.4.5 shows only one adaptive harmonic compensation block for the kth harmonic content. If say dominant harmonics need to be attenuated, then adaptive filter and gain terms of k_{adapt} are required and the net voltage reference added to the output of the PRI controller will be the sum of the voltage references generated by each of the block. Thus, depending on the number of harmonics to be attenuated, the number of blocks can be selected. Note that n in Fig.4.5 is the transformer turns ratio from secondary to primary. $i_{sec,k,t}$ is the net kth harmonic current in the secondary, which is estimated using the

LMS adaptive filter. This is mainly due to the harmonics in the magnetizing current and the dead-time effect. A single-phase PLL is used to generate the reference sine-cosine signals synchronized with the grid voltage for the adaptive filter. Next, computation of the adaptive gain k_{adapt} is discussed.

4.4 COMPUTATION OF K_{adapt} :

Based on the estimated net kth harmonic in the grid current, the voltage reference $V_{k,ref}$ is generated by multiplying the estimated harmonic with k_{adapt} . The effect of this voltage reference is that it results in an amplified voltage at that harmonic frequency at the inverter terminals and this will inject a current at that frequency in the primary side. The reflected secondary current will oppose the original current that was present in the secondary and hence there will be a net reduction in that particular harmonic in the grid current. The amount of reduction of the harmonic in grid current will depend on k_{adapt} . To calculate k_{adapt} , the control block diagram shown in Fig.4.6 is used. This block diagram is derived using Fig. 4.5 by considering the control variable to be regulated as the kth harmonic in secondary current. While deriving this harmonic control block diagram m, the fundamental current reference is set to zero.

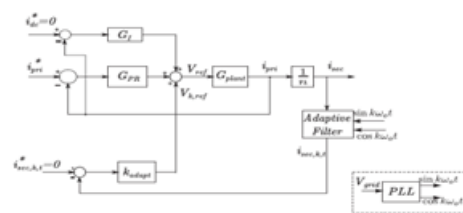


Fig. 4.5. Complete ac current control structure of the inverter.

Here, $i_{pri,k}$ is the kth harmonic in primary current, $i_{sec,k}$ is the corresponding reflected secondary current. The net kth harmonic in the secondary is given by $i_{sec,k} - i_{sec,k(0)}$, which is estimated by the adaptive filter to give $i_{sec,k,t}$. $i_{sec,k(0)}$ is the kth harmonic current flowing when there was no compensation. Let $G(s)$ be the transfer function between $v_{k,ref}$ and $i_{pri,k}$.

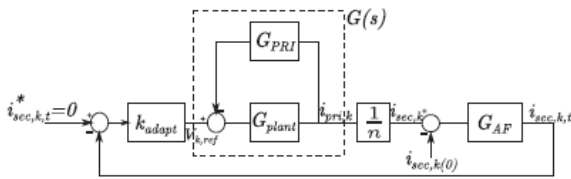


Fig.4.6. Block diagram for calculating k_{adapt} .

This can be expressed from Fig. 4.6 as in equation 4.11. Here, $G_{plant}(s)$ is the plant transfer function as given in the previous chapter.

$$G(s) = \frac{G_{plant}(s)}{1 + G_{plant}(s) + G_{PRI}(s)} \quad \dots\dots\dots 4.11$$

$G_{AF}(s)$ is the equivalent transfer function of the adaptive filter tracking k^{th} harmonic of the grid current. In order to model $G_{AF}(s)$, consider an adaptive filter which tracks a dc value in a signal. This dc tracking adaptive filter can be modeled as a first order transfer function with unity gain and with a time constant T_a which depends on the parameter μ . This transfer function is designated as $G_{AF,0}(s)$ and is given in equation 4.12. In order to obtain the transfer function of the adaptive filter tracking k^{th} harmonic, low pass to band pass transformation is used to transform equation 4.12. This gives $G_{AF}(s)$ as in equation 4.13. Thus

$$G_{AF,0}(s) = \frac{1}{1 + sT_a} \quad \dots\dots\dots 4.12$$

$$G_{AF}(s) = \frac{2s}{T_a s^2 + 2s + (K\omega_0)^2 T_a} \quad \dots\dots\dots 4.13$$

$$\frac{i_{sec,k,t}}{i_{sec,k,t}^*}(s) = \frac{K_{adapt} G(s)G_{AF}(s)/n}{1 + K_{adapt} G(s)G_{AF}(s)/n} \quad \dots\dots\dots 4.14$$

For the k^{th} harmonic, let the steady value for the transfer function in 4.14, evaluated at frequency $k\omega_0$ have a magnitude α , with $\alpha < 1$. Then

$$\left| \frac{i_{sec,k,t}}{i_{sec,k,t}^*}(jk\omega_0) \right| = \alpha \quad \dots\dots\dots 4.15$$

$$\frac{K_{adapt} G(jk\omega_0)G_{AF}(jk\omega_0)/n}{1 + K_{adapt} G(jk\omega_0)G_{AF}(jk\omega_0)/n} = \alpha \quad 4.16$$

As $G_{AF}(jk\omega_0) = 1$,

$$k_{adapt} = \frac{\alpha n}{1 - \alpha |G(jk\omega_0)|} \quad \dots\dots\dots 4.17$$

The transfer function $G(jk\omega_0)$ for harmonics can be approximated as

$$|G(jk\omega_0)| \approx \frac{1}{|G_{PRI}(jk\omega_0)|} \quad \dots\dots\dots 4.18$$

Using (4.20) in (4.19), the final expression for k_{adapt} can be obtained as

$$K_{adapt} = \frac{\alpha}{1 - \alpha} nk_p \quad \dots\dots\dots 4.19$$

SIMULATION RESULTS

BEFORE COMPENSATION

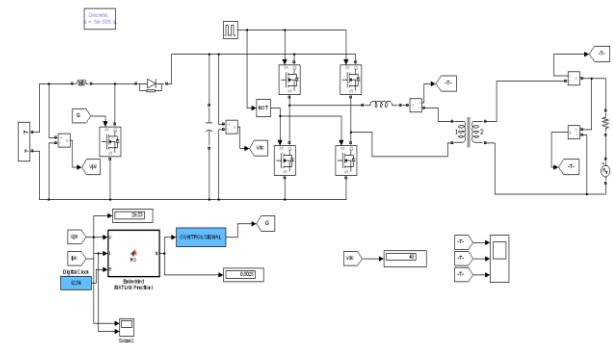


Fig 5.1: simulink model of the system with no compensation i.e. before compensation

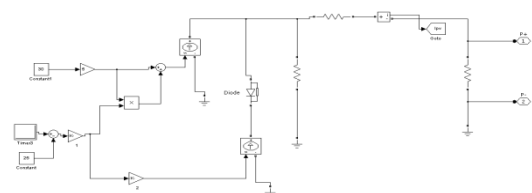


Fig 5.2: simulink model of the PV cell

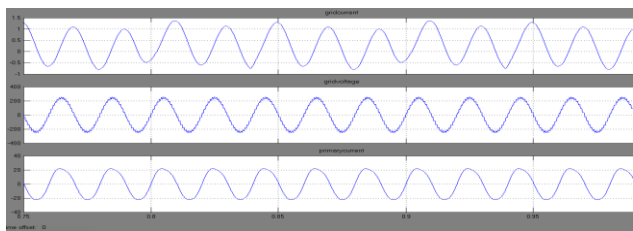


Fig 5.3: waveforms of grid current, grid voltage, primary current

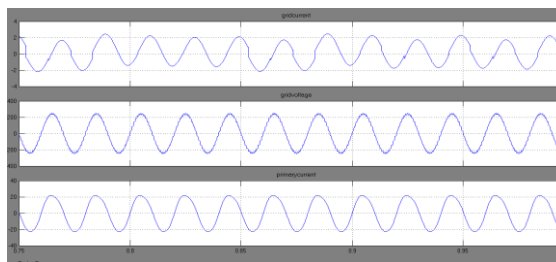


Fig 5.7: waveforms of grid current, grid voltage, primary current.

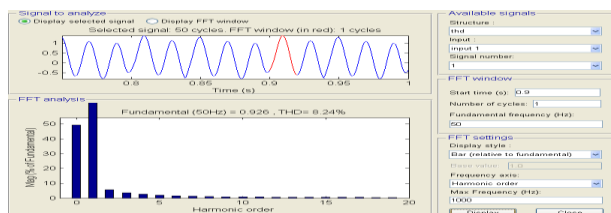


Fig 5.4: Total harmonic distortion of grid current

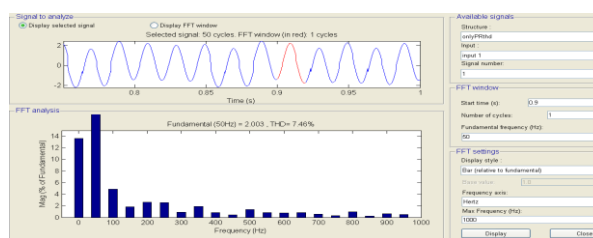


Fig 5.8: Total harmonic distortion of grid current

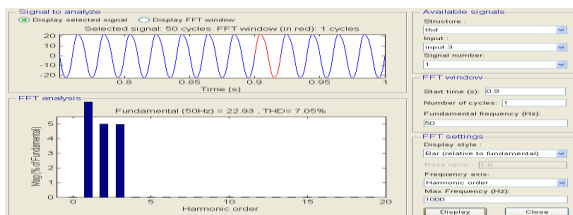


Fig 5.5: Total harmonic distortion of primary current

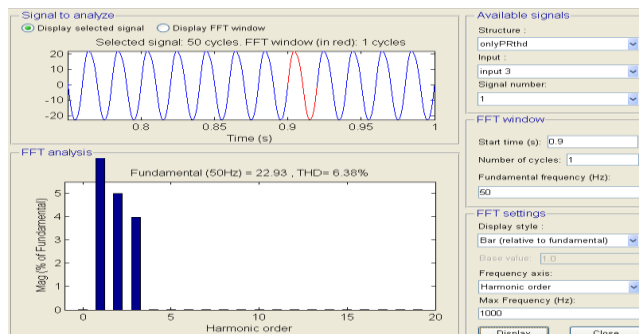


Fig 5.9: Total harmonic distortion of primary current

ONLY PR (PROPORTIONAL RESONANT) CONTROLLER IS PRESENT

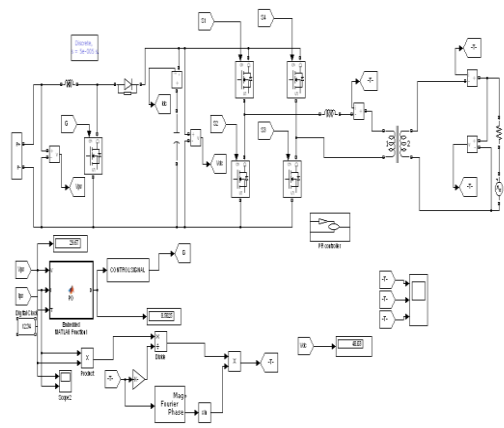


Fig 5.6: simulink model of the system with only Proportional Resonant controller

PROPORTIONAL RESONANT CONTROLLER AND LMS ADAPTIVE FILTER ARE PRESENT

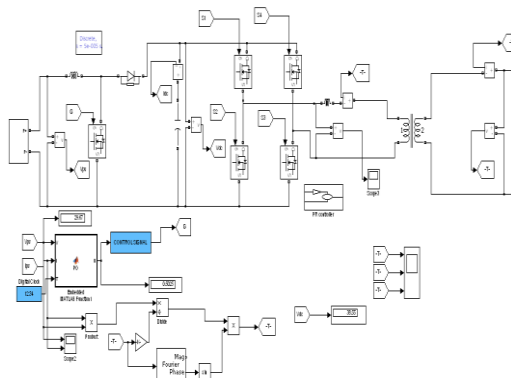


Fig 5.10: simulink model of the system with Proportional Resonant controller and LMS adaptive filter

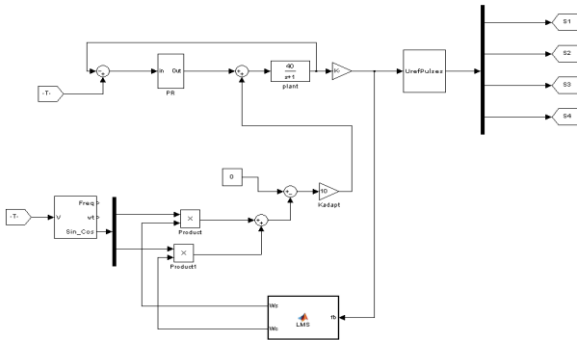


Fig 5.11: simulink model of the sub circuit system with Proportional Resonant controller and LMS Adaptive filter

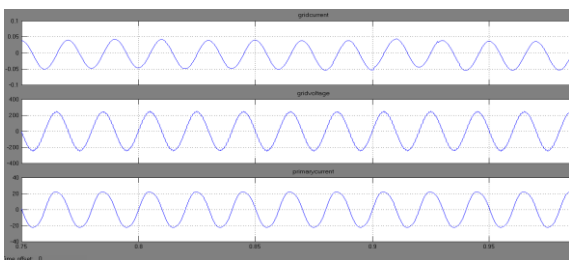


Fig 5.12: waveforms of grid current, grid voltage, primary current and secondary voltage

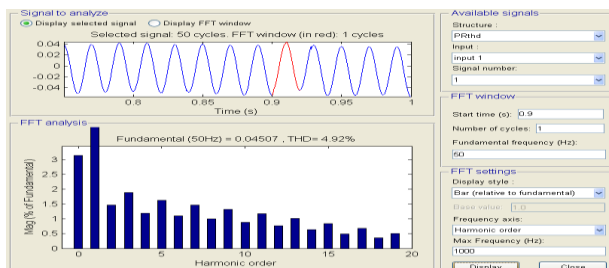


Fig 5.13: Total harmonic distortion of grid current

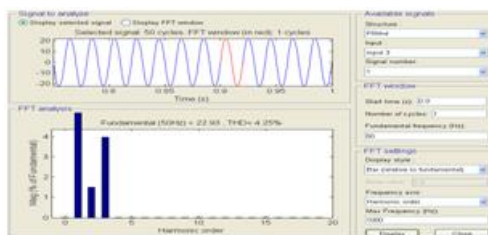


Fig 5.14: Total harmonic distortion of primary current

PROPORTIONAL RESONANT INTEGRAL CONTROLLER AND LMS ADAPTIVE FILTER ARE PRESENT

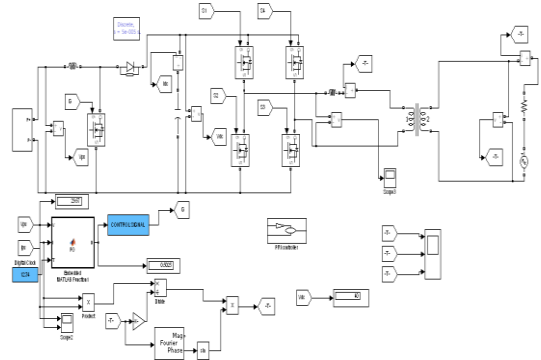


Fig 5.15: simulink model of the system with Proportional Resonant Integral controller and LMS adaptive filter.

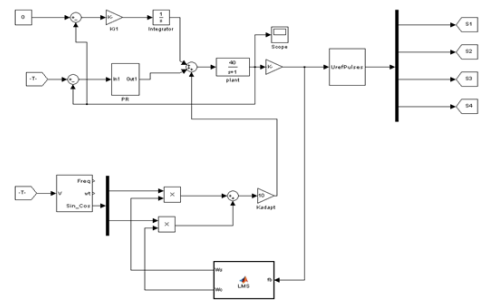


Fig 5.16: simulink model of the sub circuit system with Proportional Resonant Integral controller and LMS adaptive filter

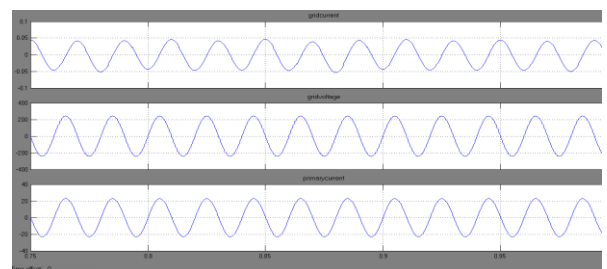


Fig 5.17: waveforms of grid current, grid voltage, primary current and secondary voltage

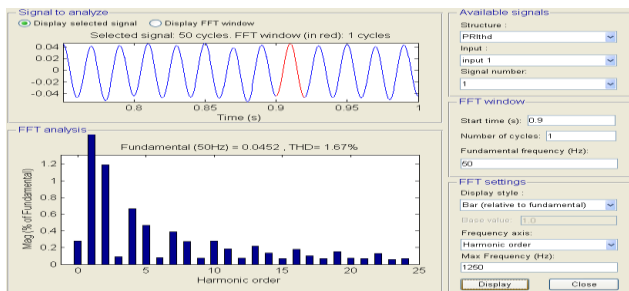


Fig 5.18: Total harmonic distortion of grid current

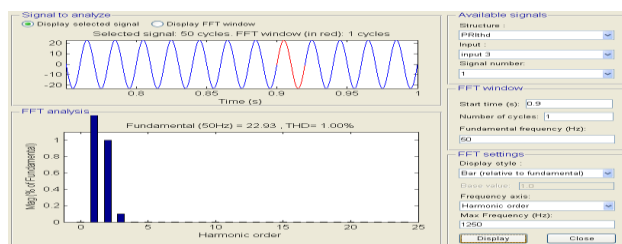


Fig 5.19: Total harmonic distortion of primary current

WITH FUZZY CONTROLLER AND LMS ADAPTIVE FILTER

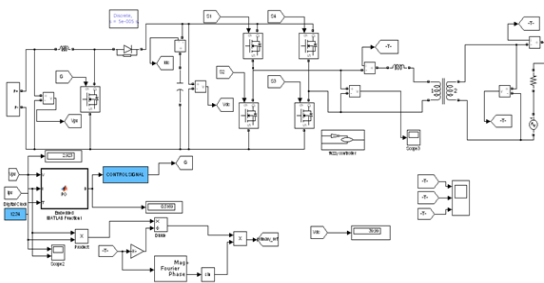


Fig 5.20: simulink model of the system with fuzzy controller and LMS adaptive filter

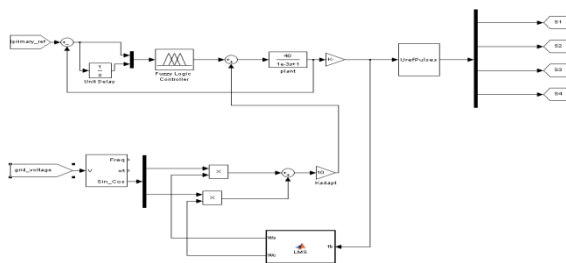


Fig 5.21: simulink model of the sub circuit system with fuzzy controller and LMS adaptive filter

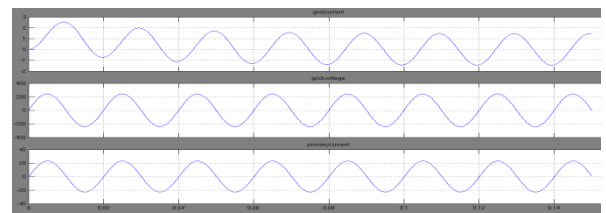


Fig 5.22: waveforms of grid current, grid voltage, primary current

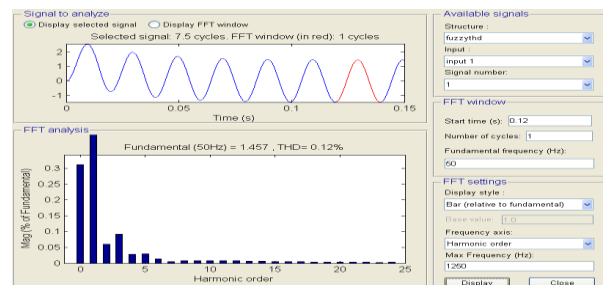


Fig 5.23: Total harmonic distortion of grid current for fuzzy controller

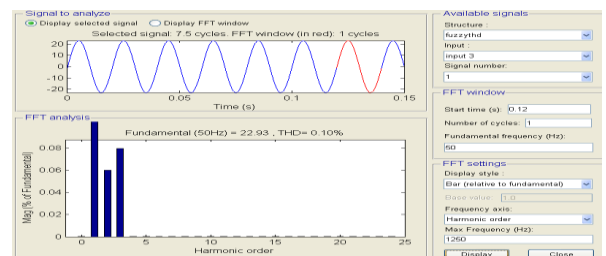


Fig 5.24: Total harmonic distortion of primary current

CONCLUSION:

Modification to the inverter current control for a grid connected single-phase photovoltaic inverter has been proposed in this work, for ensuring high quality of the current injected into the grid. The proposed method uses an LMS adaptive filter to estimate a particular harmonic in the grid current that needs to be attenuated. The estimated current is converted into an equivalent voltage reference using a proportional controller and added to the inverter voltage reference. The design of the gain of a proportional controller to have an adequate harmonic compensation has been explained.

FUTURESCOPE:

By using neural networks we can further improve the quality of the current injected into the grid by attenuating the lower order harmonics.

REFERENCES:

- [1] S. B. Kjaer, J. K. Pedersen, and F. Blaabjerg, "A review of single-phase grid-connected inverters for photovoltaic modules," *IEEE Trans. Ind. Appl.*, vol. 41, no. 5, pp. 1292–1306, Sep./Oct. 2005.
- [2] S.-G. Jeung and M.-H. Park, "The analysis and compensation of deadtime effects in PWM inverters," *IEEE Trans. Ind. Electron.*, vol. 38, no. 2, pp. 108–114, Apr. 1991.
- [3] J.-W. Choi and S.-K. Sul, "A new compensation strategy reducing voltage/ current distortion in PWM VSI systems operating with low output voltages," *IEEE Trans. Ind. Appl.*, vol. 31, no. 5, pp. 1001–1008, Sep./Oct. 1995.
- [4] A. R. Muñoz and T. A. Lipo, "On-line dead-time compensation technique for open-loop PWM-VSI drives," *IEEE Trans. Power Electron.*, vol. 14, no. 4, pp. 683–689, Jul. 1999.
- [5] A. C. Oliveira, C. B. Jacobina, and A. M. N. Lima, "Improved dead-time compensation for sinusoidal PWM inverters operating at high switching frequencies," *IEEE Trans. Ind. Electron.*, vol. 54, no. 4, pp. 2295–2304, Aug. 2007.
- [6] L. Chen and F. Z. Peng, "Dead-time elimination for voltage source inverters," *IEEE Trans. Power Electron.*, vol. 23, no. 2, pp. 574–580, Mar. 2008.
- [7] IEEE Recommended Practices and Requirements for Harmonic Control in Electrical Power Systems, IEEE Standard 519-1992, 1992.
- [8] IEEE Standard for Interconnecting Distributed Resources With the Electric Power System, IEEE Standard 1547-2003, 2003.
- [9] T. Esum and P. L. Chapman, "Comparison of photovoltaic array maximum power point tracking techniques," *IEEE Trans. Energy Convers.*, vol. 22, no. 2, pp. 439–449, Jun. 2007.
- [10] R. Kadri, J.-P. Gaubert, and G. Champenois, "An improved maximum power point tracking for photovoltaic grid-connected inverter based on voltage-oriented control," *IEEE Trans. Ind. Electron.*, vol. 58, no. 1, pp. 66–75, Jan. 2011.
- [11] T. Kitano, M. Matsui, and D. Xu, "Power sensorless MPPT control scheme utilizing power balance at DC link—System design to ensure stability and response," in *Proc. 27th Annu. Conf. IEEE Ind. Electron. Soc.*, 2001, vol. 2, pp. 1309–1314.
- [12] Y. Chen and K. M. Smedley, "A cost-effective single-stage inverter with maximum power point tracking," *IEEE Trans. Power Electron.*, vol. 19, no. 5, pp. 1289–1294, Jun. 2004.
- [13] Q. Mei, M. Shan, L. Liu, and J. M. Guerrero, "A novel improved variable step-size incremental-resistance MPPT method for PV systems," *IEEE Trans. Ind. Electron.*, vol. 58, no. 6, pp. 2427–2434, Jun. 2011.
- [14] A. K. Abdelsalam, A. M. Massoud, S. Ahmed, and P. N. Enjeti, "High-performance adaptive perturb and observe MPPT technique for photovoltaic-based microgrids," *IEEE Trans. Power Electron.*, vol. 26, no. 4, pp. 1010–1021, Apr. 2011.
- [15] P. Mattavelli, "A closed-loop selective harmonic compensation for active filters," *IEEE Trans. Ind. Appl.*, vol. 37, no. 1, pp. 81–89, Jan./Feb. 2001.